Sender Authentication for Automotive In-Vehicle Networks Through Dual Analog Measurements to Determine the Location of the Transmitter

Carlos Moreno, Sebastian Fischmeister
Department of Electrical and Computer Engineering, University of Waterloo
Waterloo, Ontario, Canada.

cmoreno@uwaterloo.ca, sfischme@uwaterloo.ca

Keywords: Cyber physical systems security, Automotive systems, Controller Area Network, Intrusion detection

Abstract: Controller Area Network (CAN) is a fundamentally insecure communications bus. Its intrinsic lack of sender authentication makes impersonation attacks a severe threat to the security of systems that rely on CAN for communication between devices. In this paper, we propose a novel technique to enforce sender authenticity on a CAN bus. The technique is reliable, robust, and reasonably easy and inexpensive to implement, as it relies on non-clonable physical characteristics of the transmitted signals. In particular, we measure the analog signal at two different locations on the CAN bus physical wire; the signal corresponding to the transmitted message travels through the wire at a certain speed, which allows us to determine the physical location (i.e., position along the wire) of the transmitter as a function of the relative delay between the two analog measurements. Our work includes an experimental evaluation on an actual vehicle, with results that suggest that the technique is effective and practical.

1 Introduction

Controller Area Network (CAN) is a fundamentally insecure communication bus. Historically, this has not been a critical issue, since automotive vehicles had little or no connectivity to the outside world, and cybersecurity was not as critical or widespread as it is in the modern world. However, modern vehicles include a high level of connectivity, including the Internet; moreover, the prospect of autonomous vehicles makes cybersecurity a critical aspect in modern automotive vehicles.

Security of automotive vehicles has received a great deal of attention in recent years, with some works studying and reporting the potential vulnerabilities (Checkoway, S. et al., 2011; Koscher et al., 2010; Petit and Shladover, 2015; Mukherjee et al., 2016), some works reporting concrete practical attacks, most notably the Jeep Cherokee hack by Miller and Valasek (Miller and Valasek, 2015; Miller and Valasek, 2016), and several works proposing strategies and guidelines for securing automotive vehicles (McAfee, 2015; Pike et al., 2015; SAE, 2016).

Problem Statement

Several of the above mentioned works highlight the importance of sender authentication (rather, the lack thereof) as one of the critical attack vectors. In particular, the work by Miller and Valasek (Miller and Valasek, 2015) demonstrate the realistic nature of this threat, where they compromised a vulnerable Electronic Control Unit (ECU) with unintended connectivity to the Internet, and used it to send messages impersonating other ECUs.

This leads to the motivating problem for our work, which is that of sender authentication on a Controller Area Network. Specifically, given an ongoing transmission, determine as early as possible whether the transmission is actually sent by the purported sender (i.e., by the sender identified by the data in the transmission).

Related Work

There have been several attempts to tackle the problem of sender authentication on a CAN bus. These include approaches based on the use of cryptography, such as (Van Herrewege et al., 2011; Groza et al., 2017). However, the broadcast nature and relatively low bandwidth of the CAN bus limit the applicability of these techniques. Moreover, heterogeneous, commercial off-the-shelf (COTS) devices are commonly used by automobile designers. This makes it difficult to set up all the devices to share common secrets

to be used for symmetric-key cryptographic primitives. Alternative approaches are based on fingerprinting some physical characteristic(s) of the transmitting ECU. Timing-based detection of impersonating ECUs was proposed in (Cho and Shin, 2016). However, as shown by (Sagong et al., 2018), these timing characteristics can be fingerprinted and emulated by an attacker, entirely bypassing the protective measure. We refer to this as a *profile-and-mimic* attack. Voltage-based sender identification techniques have been recently proposed, with the work by Murvay and Groza (Murvay and Groza, 2014) being the first one proposed, followed by Viden (Cho and Shin, 2017), and a refined implementation of Viden's idea in Scission (Kneib and Huth, 2018). Although to the best of our knowledge no attacks have been proposed that defeat these techniques, it is conceivable, even intuitive, that they are also vulnerable to profile-and-mimic attacks — an attacker with temporary physical access to the CAN bus could place a transmitter that uses a custom-made analog CAN driver that is able to inject an arbitrary waveform on the CAN bus. This is even more plausible when we observe that these techniques do not use the complete analog waveform of transmissions, but simply extract some statistical characteristics of the voltage, making it easier to emulate by an attacker.

Our Contributions

We propose a novel technique to enforce sender authenticity on a CAN bus. The technique is based on measuring the analog transmitted signal at two different locations on the CAN bus physical wire; the signal corresponding to the transmitted message travels through the wire at a certain speed, which determines unique propagation delays from a given physical location of the sender (i.e., position along the wire) to each measuring device. With two measurements, the system can *biangulate* [1] to determine the physical location of the transmitter as a function of the relative delay between the two analog measurements.

Our proposed approach exhibits some important and somewhat unique advantages:

- The technique is not vulnerable to profile-and-mimic attacks, as it relies on the propagation timing of the transmitted signals as they travel through the physical wire. These characteristics cannot be reproduced by a sender at a different physical location on the bus. Simply put: the actual physical location where a transmission originates cannot be mimicked by an ECU transmitting from a different physical location. Thus, a profile-and-mimic attack is simply not possible by a remote attacker that compromises some other ECU(s) on the same CAN bus.

  For an attacker with physical access to the CAN bus, they could conceivably place the attacking ECU in close proximity to the victim ECU. However, it may be straightforward to design the physical wiring of a vehicle in a way that makes this task difficult — indeed, the wiring of modern vehicles is so complex that this could already be the case even if the manufacturer did not intend to make it difficult for a third-party to connect to the CAN bus at a location in close proximity to a target ECU.
- The technique can be easily implemented with analog processing that drastically reduces the computational power requirements to implement the necessary processing. Although our experimental evaluation was based on digital signal processing, we discuss the design based on analog processing and present a sketch of its implementation in Section 3.2.5.
- Our technique can be effectively used for attacks prevention, and not just detection: the timing characteristics that determine the physical location of the sender are available as early as at the first edge of the start bit of the transmission. Thus, an attack prevention system can disrupt and effectively inhibit the forged transmission before it is completed. We will discuss this in more detail after we discuss the characteristics of CAN transmissions in Section 2.1.

Our work includes an experimental evaluation on an actual vehicle, a Lexus RX-450H. The results suggest that our proposed approach is feasible and effective.

2 Background

This section presents some background notions relevant to this work, including details on the CAN bus as well as signals propagation through transmission lines.

2.1 Controller Area Network

Controller Area Network (CAN) is a serial communication protocol with broadcast (bus) topology (Robert Bosch GmbH, 1991). Its physical layer consists of a twisted-pair cable where a binary signal is transmitted using differential signaling. The two signals are denoted CAN_H and CAN_L (CAN High and Low, respectively). Typically, the "rest" state of the bus — a logical 1 — is given by both CAN_H and CAN_L at

[1] We use the term biangulate by analogy to triangulate: biangulation is to a one-dimensional location as triangulation is to a two-dimensional location.

the middle of the voltage range, 2.5 V, and a logical 0 is represented by the CAN_H signal at 2.5 V + Δv and the CAN_L signal at 2.5 V − Δv, where Δv can be implementation specific. Additional details or a comprehensive list of configurations are not relevant to understanding our work.

The bus operation is based on a "wired AND" mechanism where any device connected to the bus can either assert a logical 0, or release the bus to implicitly bring its logical state to 1 (unless some other device is asserting a logical 0). Thus, a CAN driver typically features two "open-collector" connections to drive its outputs, as shown in Figure 1.

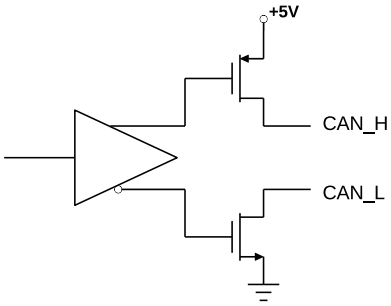

Figure 1: Simplified Diagram of a CAN Driver.

Arbitration of the bus is done by the devices themselves: the ID field in a CAN frame (see Figure 2) represents the priority of the transmission.[2] Lower numeric values represent higher priority. As a device *D* transmits its ID, it monitors the bus. Since the ID is transmitted MSB to LSB, a logical 0 on the bus while *D* transmits a logical 1 means that some other device is transmitting a lower ID value, and thus has higher priority. This condition causes the device *D* to abort its transmission and release the bus. We omit any details about retransmission attempts and other related issues, as these are not relevant to our work.

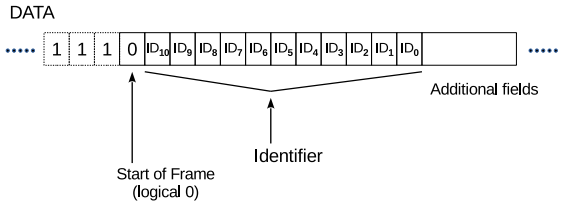

Figure 2: Start of a CAN Base Frame.

[2] For simplicity, we only show the Base frame format, with an 11-bit ID; the principle applies identically to extended frames (29-bit ID), but the details are not relevant.

2.2 Transmission Lines

In the context of electronic circuits, electrical signals are waves that travel through transmission lines — conduits that guide the propagation of the signal. Simple examples of transmission lines are cables, including coaxial cables and twisted-pair.

Transmission lines have a so-called *characteristic impedance*, which affects, among other things, the speed at which the signal travels (Blood, W. R., Jr., 1988). Like with mechanical waves or light, a discontinuity in the characteristic impedance causes part or all of the wave to be reflected. This can be visualized from the perspective of energy transmission. An unterminated (open) transmission line involves inability to maintain the signal propagation after a certain point; the signal is thus reflected. On the other hand, a resistive element with a resistance value that matches the characteristic impedance of the wave leads to the energy being absorbed without reflection.

Twisted-pair cables used in CAN have a nominal characteristic impedance of 120 Ω. Thus, the bus is *terminated* on both endpoints with 120 Ω resistors, to minimize reflections. This is done for signal integrity purposes, as reflected signals would be superposed to the original signal causing spurious noise-like artifacts. Also related to this aspect is a detail that is relevant to the operation of our proposed technique: if a device "tapping" into a twisted-pair cable transmits a signal, this signal travels *in both directions*, moving outwards from the point where the transmission originates. These aspects are illustrated in Figure 3.

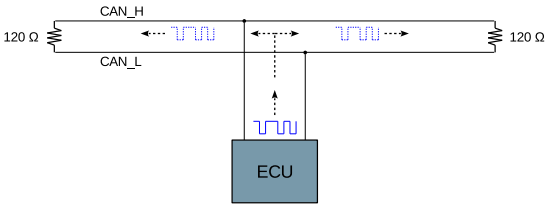

Figure 3: CAN Transmission Line with Termination Resistors.

The speed of signals in unloaded transmission lines can be typically in the order of $\frac{1}{2}c$ or $\frac{1}{3}c$, where c is the speed of light in vacuum. This speed can be reduced by a considerable factor if the line is loaded, due to the input capacitance of the connected devices (Blood, W. R., Jr., 1988). In our experimental measurements, we observed a propagation speed in the order of $\frac{1}{10}c$ (this is an estimate, as the vehicle's specifications available to us do not provide exact lengths of the cables).

3 Our Proposed Technique

This section describes the details of our proposed technique, including our threat model and assumptions, operation and novelty of the technique, and a description of the analog processing scheme to reduce the computational requirements of our technique.

3.1 Threat Model and Assumptions

In our attack model, we assume that an attacker may be able to exploit some security vulnerabilities on some ECUs, and want to use these to transmit crafted data that would disrupt the functionality of the system as a whole. Such transmissions in general require specific IDs, which ties them to specific ECUs.

To simplify the presentation, we will assume that the attacker has a particular target ECU, denoted E_T, that is otherwise secure (i.e., the attacker does not have access to any exploitable vulnerabilities in E_T) and wants to send crafted data that is logically valid but may cause E_T, and presumably the vehicle, to deviate from normal/correct operation. For example, E_T could be the engine control unit, and the attacker could use other (compromised) ECU(s) to inject false speed and temperature data that may result in overheating or damage to the engine.

Our threat model includes an attacker with the following concrete capabilities:

- **Control existing ECUs:** An attacker can compromise (in particular, hijack control) some other ECU(s) on the same CAN bus where the target ECU, E_T, is. For example, some ECU E_B could exhibit unintended connectivity combined with vulnerabilities that allow an attacker to execute arbitrary code on E_B or even reprogram its firmware.
- **Add ECU(s) to the bus:** An attacker may gain temporary physical access to the CAN bus where E_T is, and connect an arbitrary device (e.g., an ECU with custom firmware designed by the attacker) to the bus.

3.1.1 Assumptions and Limitations

Our work relies on the following assumptions:

- **ECU capabilities:** Any ECU can transmit arbitrary data with arbitrary IDs. Though this does not occur during normal operation, this assumption emphasizes the aspect that a compromised ECU E_C can, under the attacker's control, transmit any arbitrary message, including any arbitrary ID.
- **Secure Monitor:** An implementation of our proposed technique is assumed to be secure and tamper-proof, possibly physically isolated from any CAN bus and any of the vehicle's ECUs.
- **Classes of attacks detected:** Our proposed technique is limited to detect impersonation attacks. If an ECU E_C transmits malicious data with IDs that legitimately correspond to E_C, our system will not detect any anomalous or suspicious behavior.

3.2 Proposed Technique – Biangulation to Authenticate Sender

Figure 4 illustrates the basic idea behind our proposed technique. The ECU transmits a message which propagates to the left (wave ω_L) and to the right (wave ω_R). Two analog differential amplifiers at two different positions on the bus measure each of these signals, obtaining differential voltages v_L and v_R. In the diagram, the amplifiers are near the bus' endpoints, which is the optimal configuration; however, as we will discuss shortly, other configurations may also work.

In the example in Figure 4, we see that the signal ω_L arrives at its corresponding analog differential amplifier before the signal ω_R. This indicates that the transmission originates on the left half of the CAN bus. If we assume a constant propagation speed (independent of the position along the cable), then:

Let v be the speed (magnitude) at which the signals travel through the CAN bus; let x_0 be the position at which the ECU connects to the bus; let x_L and x_R be the positions of the connections to the left and right differential amplifiers, respectively (by convention, $x_L < x_0 < x_R$); let τ_L and τ_R be the additional time that it takes from the connection at the CAN bus to the inputs of the time shift measurement subsystem (these are fixed values, since the lengths and geometry of the wires involved and the propagation delays through the differential amplifiers are fixed). Then, the time shift $\Delta t \triangleq t_R - t_L$ is:

$$\begin{aligned} \Delta t &= \left(\frac{x_R - x_0}{v} + \tau_R\right) - \left(\frac{x_0 - x_L}{v} + \tau_L\right) \\ &= \frac{x_R + x_L - 2x_0}{v} + \tau_R - \tau_L \end{aligned} \quad (1)$$

The time shift is an injective function of x_0, the position of the ECU on the bus. Thus, the position x_0 is a function of the time shift. In the more general case of a speed that is a function of the position x along the cable, $v(x)$, the time shift is:

$$\Delta t = \int_{x_0}^{x_R} \frac{1}{v(x)}\,dx - \int_{x_L}^{x_0} \frac{1}{v(x)}\,dx + \tau_R - \tau_L \quad (2)$$

Since $v(x) > 0$, in this general case the time shift is also an injective function of the position x_0. This is the case since the first integral term, corresponding to the cable fragment on the right, is a monotonically decreasing function of x_0, and the second integral term

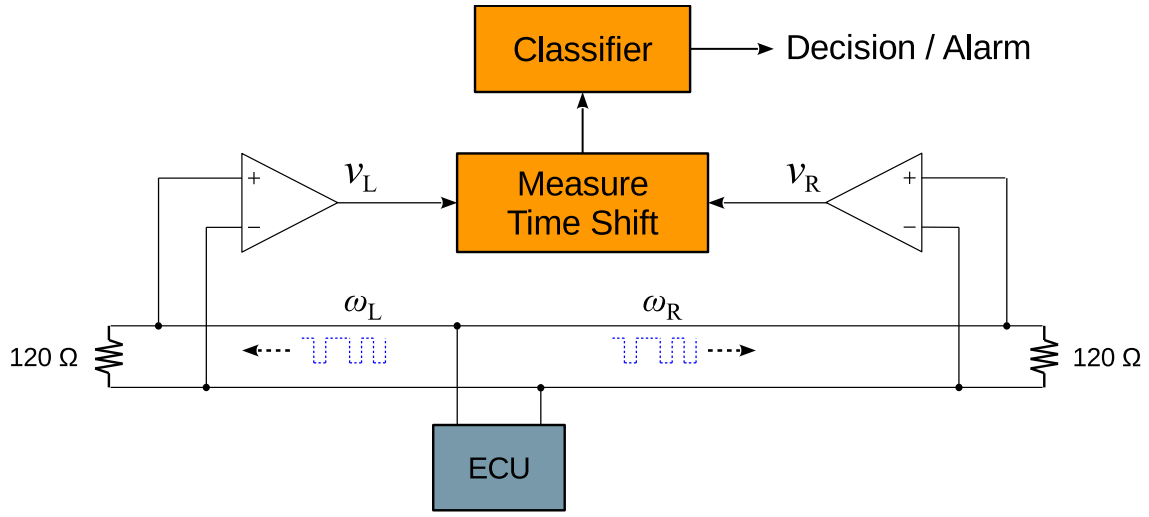

Figure 4: Biangulation System Diagram.

is a monotonically increasing function of x_0. Like in the simplified case of constant speed, the position x_0 is a function of the time shift Δt — albeit, an exceedingly difficult function to compute in practice.

This brings us to an important aspect in a practical implementation of our technique, including our prototype implementation for this work: we *do not need* to explicitly obtain the value of x_0 given a measurement of the time shift for a given transmission. The fact that x_0 is a function of Δt means that we can profile this function through measurements of the time shift for messages sent by each ECU. Thus, the classifier is a simple algorithm that compares the given time shift against a set of ranges. These ranges are obtained during a training phase where we profile the time shifts for the various ECUs.

3.2.1 Optimal Location of the Measurement Points

The optimal location of the measurement points x_L and x_R is given by any configuration such that $x_L < x_k < x_R \; \forall k \in [1, N]$, where x_k is the position of the k^{th} ECU and N is the number of ECUs on the bus. This is clearly the case: if ECUs are connected outside the cable segment between x_L and x_R, then it is no longer the case that the time shift is an injective function of the position where a transmission originates. More formally, if the domain of this function is not restricted to the interval between x_L and x_R, then the function is not injective. Thus, the position is not a function of the measured time shift. It is straightforward to show that this is the case: signals originating at $x_R + x$ ($x > 0$) produce the same time shift, independently of x. Similarly for signals originating at $x_L - x$.

If at most one ECU on each side is allowed outside the interval (x_L, x_R), then the configuration still works. However, x_L and x_R further away means that the positions of the ECUs (and thus the values of the time shifts) are spread out over a larger range, which leads to potentially better accuracy of the detector.

3.2.2 Attack Prevention

As briefly mentioned in Section 1, our technique can be used to block transmissions subject to sender impersonation, and not just detect them. The information necessary to determine the time shift — and thus the legitimate sender — is available as early as at the first edge of the start bit. The claimed sender is known at the end of the ID field. Thus, a mismatch is detected at this point. Given the "wired AND" nature of the bus, the detector can disrupt the remainder of the message to make it invalid and make all other ECUs discard it. This can be accomplished, e.g., by asserting one or several logical 0's to cause the checksum field to mismatch the message's contents.

Engineers implementing this idea should exercise extreme caution. False positives or otherwise incorrect decisions to block transmitted messages could have severe safety implications, depending on the criticality of the blocked messages.

3.2.3 Optimizations

To measure the time shift, our implementation as part of this work simply digitized both signals (v_L and v_R) and processed them off-line. The sampling has to be done at a high enough rate to be able to measure the small time shifts. This imposes a computational workload that may be too heavy for a practical implementation. The following subsections present two

approaches to optimize the technique that are reasonably easy to implement.

3.2.4 Sampling During a Small Interval Around the Signal's Edge

A key observation that can lead to an important optimization is that we only need to process the digitized signals during a short interval around the edge. For example, an external simple edge detecting circuit could trigger the sampling and data processing. Alternatively, the system could sample continuously at high frequency, sending the samples through a (circular) FIFO buffer, enabling the processing only when an edge is detected.

3.2.5 Analog Processing

Another important optimization could result from the use of analog circuitry to measure the time shift. We start with a simplified model of the signals, with $v_{\mathrm{L}}(t) = 2\Delta v\ u(t-t_0)$ and $v_{\mathrm{R}}(t)$ similarly defined. $u(t)$ is the unit step function:

$$u(t) = \begin{cases} 0 & t \leqslant 0 \\ 1 & t > 0 \end{cases} \tag{3}$$

Without loss of generality, let us assume that the ECU is on the left half of the cable (like in the example in Figure 4), and let us define $t = 0$ as the time of arrival of the edge (a transition) of v_{L} to the time measurement subsystem. Then:

$$\Delta t \ \propto \ \int_0^{\delta} \left(v_{\mathrm{R}}(t) - v_{\mathrm{L}}(t)\right)\ dt \tag{4}$$

for some δ sufficiently small that the integration interval does not cover more than one edge, and also sufficiently large that it covers the edges in both $v_{\mathrm{R}}(t)$ and $v_{\mathrm{L}}(t)$.[3]

One can simply approximate the integral with a resistor-capacitor circuit, as illustrated in Figure 5, observing that a strict integration operation is not required; the relevant characteristic of the integral is that during the time shift, when $v_{\mathrm{R}}(t) - v_{\mathrm{L}}(t) > 0$, the integrated signal's value increases at a constant rate. Given our goal of exploiting the fact that the position of the sender is a function of the measured time shift, we only require a monotonically increasing transformed signal. This guarantees that the value of that transformed signal is an injective function of the time shift, and thus the time shift is a function of that value. The output of a resistor-capacitor circuit

[3] Given the speeds of the CAN bus (up to 1 Mbps), the time shift is always much smaller than the duration of a bit in the transmission.

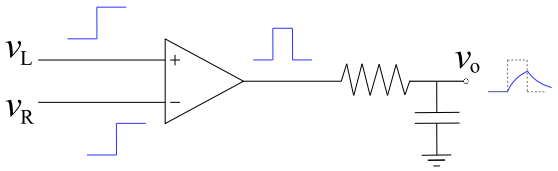

Figure 5: Resistor-Capacitor Circuit to Approximate Integration.

meets this requirement, as illustrated in Figure 5. In the figure, the time shift is a function of the peak value of the output signal v_o. If the shift is reversed (i.e., if v_{L} is delayed with respect to v_{R}), then v_o would take negative values and the value with highest magnitude is what determines the time shift.

4 Experimental Evaluation

In this section we describe our experimental setup, and present and discuss the results.

4.1 Setup

The main goal of our experimental evaluation is to confirm the feasibility and practicality of our proposed technique. Thus, we implemented the analog measurement devices (custom designed for this work), and created a proof-of-concept implementation of the time shift measurement subsystem. We did not explicitly implement the classifier / detector, as the results for the time shift measurement implementation directly provide a reasonable prediction of the performance of such a classifier.

The fundamental unknown that our experimental evaluation needs to answer relates to the precision of the measurements in a real vehicle, given limiting factors such as variations in the transmission line and speed, measurement noise and resolution, etc. This aspect determines the applicability of our technique in practice, since it determines how narrowly our technique can obtain the position of the transmitting ECU, and thus, whether ECUs can be distinguished from each other based on their positions.

4.1.1 Vehicle Instrumentation

We instrumented one of the CAN buses of a Lexus RX-450H with two analog differential amplifiers. We selected the vehicle's CAN 2 bus, since that one is accessible at a reasonably low level of difficulty, and without an excessive risk to result in damage to the vehicle. CAN 2 runs from the dashboard (left and below the steering wheel) to the back of the vehicle.

Approximate measurements indicate a distance of 2 m between the two analog differential amplifiers.

The largest time-shift measured in the experiments was around 70 ns, suggesting an average speed of $\frac{1}{10}c$ (assuming that this largest time shift corresponds to the distance between the two analog measurements).

For the purpose of demonstrating applicability of the technique at low cost, we used a Texas Instruments OPA211 operational amplifier in a standard differential amplifier configuration (Horowitz and Hill, 2015). To confirm that the bandwidth of this amplifier (45 MHz, with a slew-rate of 27 V/μs) is sufficient to faithfully reproduce the transitions (sharp transitions involve significant contents of high frequencies), we repeated the measurements using a high-frequency current feedback operational amplifier, the Analog Devices ADA4927, with a bandwidth of 2.3 GHz and a slew-rate of 5000 V/μs. The design of our high-speed amplifier included higher-grade circuit board design and manufacturing, including impedance control. The measurements with this ultra high-speed amplifier resulted in essentially identical time-shift values, compared to those obtained with the lower-end alternative. This confirmed the applicability of lower cost solutions to implement our technique.

The output of the analog measurements are sent to 50 Ω coaxial cables connecting to the inputs of an AlazarTech ATS9462 Digitizer card, with two-channel simultaneous capture at 16-bit and a maximum sampling rate of 180 Msps. In practice, due to internal bus and hard disk bandwidth, we found a safe upper limit of 100 Msps, which is the capture speed we used in our experiments.

The cables going from the CAN bus connections to our amplifier boards had matching lengths, and the coaxial cables were identical (commercial off-the-shelf 6-feet cable assemblies). This means that in our setup, the values τ_L and τ_R were identical. This is not necessary and does not improve the effectiveness or any metrics of the technique, but it can potentially help facilitate verification of certain results, by removing one unknown (the difference $\tau_R - \tau_L$) from the model. Figure 6 shows a photograph of our board and its connections in our setup.

4.2 Results

With the setup as described in Section 4.1, we captured a little more than 800 000 CAN frames, during a total time of approximately 2 hours. These captures include transmissions with the vehicle off, vehicle idling (parked), and while driving the vehicle, including inside our campus and on public roads. During all of the periods, we tried to exercise as many vehicle features as possible: while parked, we repeatedly opened and closed all windows, adjusted the seats positions, changed the A.C. and fan speed settings. During the driving period, in addition to the normal activity, we enabled the driver-assistance features: adaptive cruise-control, parking assist (when parking, we intentionally passed close to objects, and approached front and rear objects such that the parking assist alarms would beep). This was done with the goal to make as many different ECUs as possible transmit data that we would capture.

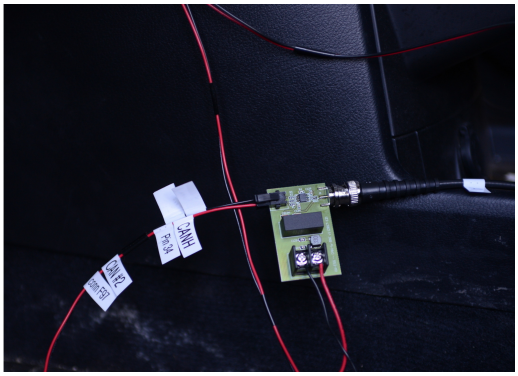

Figure 6: Analog Measurement Board and Connections.

We isolated the frames from the captured analog waveforms, and decoded them (only the IDs) through custom programs that we created for these experiments. This was clearly the simplest approach: using a separate tool to capture and decode CAN messages would have introduced the difficulty of synchronizing the output of such tool to our analog captures. Figure 7 shows an example of the start of a CAN frame, including both analog measurements (corresponding to v_L and v_R, labeled as per Digitizer input channel) to show the time shift (in this case, approximately 7 samples, corresponding to 70 ns).

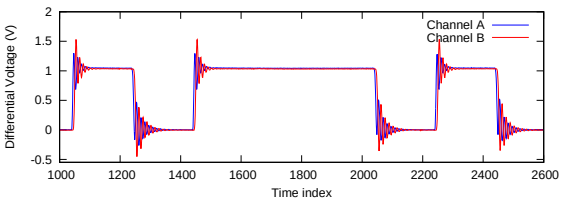

(a) Start of CAN Frame – Dual Measurement

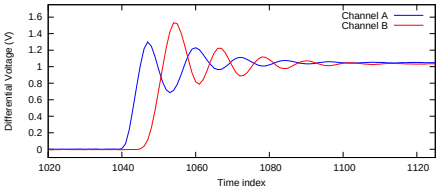

(b) Detail of Start Bit Showing Time Shift

Figure 7: Example of Analog Capture of a CAN Frame.

To determine the time shift, we used the numerical approximations of the second derivatives to find the inflection point in each of the measurements (Press et al., 1992). The inflection point provides a precise representation of the position of the edge. We interpolated the values of the second derivatives, allowing us to determine the location of the inflection points with sub-sample resolution.

Vehicle's manufacturers in general (and in our specific case as well) do not disclose information about CAN transmissions. In particular, the correspondence between ECUs and CAN frame IDs is not publicly known. However, since the ID field is used for bus arbitration, we have the guarantee that each ID uniquely corresponds to an ECU (that is, different messages with the same ID field are guaranteed to be transmitted from the same ECU [4]). We observe that the converse does not hold: one ECU can be the sender that corresponds to multiple IDs.

Thus, we measured the time shift for each transmission and grouped them by ID to compute mean and standard deviation. The standard deviation relates to the precision of the measurement, and ultimately defines the range of uncertainty for the position of the sender. Since one ECU can have multiple IDs associated to it, we clustered the time shifts for IDs where ranges had a significant overlap. Table 1 shows the results for the four observed clusters. The standard

Table 1: Statistics for Each Cluster of Time Shifts

Cluster	# of Samples	Mean (ns)	Std. Dev. (ns)	Std. Dev (cm)
1	939	-62.9357	3.42349	10.2705
2	55357	2.28171	3.7476	11.2428
3	4067	41.6689	1.99615	5.98845
4	754202	68.9884	2.22483	6.67448

deviation is reported both in time units and in space units, using the estimated average speed, $\frac{1}{10}c$. This relates to the uncertainty in the location of the ECU. Table A1 in Appendix A shows the complete listing of mean and standard deviation for each distinct ID.

Figure 8 shows the *normalized* histograms for each of the clusters. We normalized them since, as can be seen in Table 1, the number of samples for cluster 4 is large compared to the other clusters, so those would not be visible in the combined histogram.

The results confirm the feasibility of our proposed technique: our proof-of-concept implementation is able to narrow down the position of the sender to within 20 or 30 cm. Regarding the vehicle's configuration, the fact that the clusters are narrow relative to the distance to other clusters means that our technique can reliably distinguish senders from each of these four sources with high accuracy. For example, for the two closest clusters (3 and 4), a boundary value in the middle point is at more than 6 standard deviations from either mean; hence the probability of misclassification is negligible. Moreover, the histograms suggest that each cluster does indeed correspond to a single location of the sender, as each cluster looks reasonably close to a single bell shape.

[4] Under normal operation, without malicious devices impersonating other ECUs.

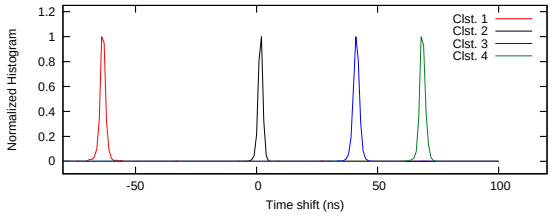

Figure 8: Normalized Histograms for the Time Shift Clusters.

5 Discussion and Future Work

The main difficulty with the experimental evaluation was the lack of available documentation and details about the CAN bus and ECUs. Vehicle manufacturers in general do not disclose any details on these. In particular, the connection points (x_{L} and x_{R}) were not under our control, as we were restricted in terms of which locations were physically accessible without causing damage to the vehicle's wiring or body.

However, the results do show the potential capabilities of our technique: automotive engineers implementing this technique could use the internally available information to guide the design, and even could adapt the design and configuration of a vehicle's CAN bus to facilitate or to maximize the effectiveness of our technique. For example, a critical ECU (an ECU for which false positives are critical), could be placed such that the distance to other ECUs is maximized.

In terms of future work, many interesting questions and avenues for future research arise from this work. In particular:

- **J-1939:** Heavy vehicles use the J-1939 standard protocol (a layer above the CAN protocol). With this protocol, we would have the advantage of being able to decode the protocol and count on the "ground truth" for the experimental evaluation.
- **Improvements in performance:** We will investigate the use of multiple edges to average multiple estimates of the time shift and obtain a more accurate measurement. Though the system can determine the time shift upon the falling edge of the start bit, it must wait until the ID has been

transmitted entirely before it can output a decision. Thus, all of these edges can be exploited to take multiple measurements.

- **On-the-fly operation:** This work produced a proof-of-concept implementation that captures data to be processed off-line. We will also work towards an implementation with on-the-fly operation. This will provide a much deeper insight into the practicality of our technique.

6 Conclusions

We presented a novel technique to identify the sender in Controller Area Networks. The technique is highly effective, as it relies on physical characteristics of an ECU's transmission that an attacker attempting to impersonate the ECU cannot mimic. This constitutes an important advantage over state-of-the-art approaches, that are conceivably vulnerable to profile-and-mimic attacks. The work includes an experimental evaluation that confirms the feasibility and practicality of our proposed technique.

Acknowledgements

The authors would like to thank Lorin Maran for his valuable assistance with the vehicle's instrumentation. We would also like to thank Arthur Chung for his valuable guidance and discussions regarding our high-frequency board design.

REFERENCES

Blood, W. R., Jr. (1988). MECL System Design Handbook (HB205/D, Rev. 1A).

Checkoway, S. et al. (2011). Comprehensive Experimental Analyses of Automotive Attack Surfaces. In *USENIX Security Symposium*.

Cho, K.-T. and Shin, K. G. (2016). Fingerprinting Electronic Control Units for Vehicle Intrusion Detection. In *USENIX Security Symposium*.

Cho, K.-T. and Shin, K. G. (2017). Viden: Attacker Identification on In-Vehicle Networks. In *Proceedings of the 2017 ACM SIGSAC Conference on Computer and Communications Security*, pages 1109–1123. ACM.

Groza, B., Murvay, S., Herrewege, A. V., and Verbauwhede, I. (2017). LiBrA-CAN: Lightweight Broadcast Authentication for Controller Area Networks. *ACM Transactions on Embedded Computing Systems*, 16(3):90:1–90:28.

Horowitz, P. and Hill, W. (2015). *The Art of Electronics*. Cambridge University Press, Third edition.

Kneib, M. and Huth, C. (2018). Scission: Signal Characteristic-Based Sender Identification and Intrusion Detection in Automotive Networks. In *ACM SIGSAC Conference on Computer and Communications Security*. ACM.

Koscher, K., Czeskis, A., Roesner, F., Patel, S., Kohno, T., Checkoway, S., McCoy, D., Kantor, B., Anderson, D., Shacham, H., et al. (2010). Experimental Security Analysis of a Modern Automobile. In *IEEE Symposium on Security and Privacy*, pages 447–462. IEEE.

McAfee (2015). Automotive Security Best Practices.

Miller, C. and Valasek, C. (2015). Remote Exploitation of an Unaltered Passenger Vehicle.

Miller, C. and Valasek, C. (2016). Advanced CAN Injection Techniques for Vehicle Networks.

Mukherjee, S., Shirazi, H., Ray, I., Daily, J., and Gamble, R. (2016). Practical DoS Attacks on Embedded Networks in Commercial Vehicles. In *International Conference on Information Systems Security*, pages 23–42. Springer.

Murvay, P.-S. and Groza, B. (2014). Source Identification Using Signal Characteristics in Controller Area Networks. *IEEE Signal Processing Letters*, 21(4):395–399.

Petit, J. and Shladover, S. (2015). Potential Cyberattacks on Automated Vehicles. *IEEE Transactions on Intelligent Transportation Systems*, 16(2):546–556.

Pike, L., Sharp, J., Tullsen, M., Hickey, P. C., and Bielman, J. (2015). Securing the Automobile: a Comprehensive Approach. In *Embedded Security in Cars (ESCAR) Conference*.

Press, W., Teukolsky, S., Vetterling, W., and Flannery, B. (1992). *Numerical Recipes in C*. Cambridge University Press, Second edition.

Robert Bosch GmbH (1991). CAN Specification, Version 2.0.

SAE (2016). Cybersecurity Guidebook for Cyber-Physical Vehicle Systems.

Sagong, S. U., Ying, X., Clark, A., Bushnell, L., and Poovendran, R. (2018). Cloaking the Clock: Emulating Clock Skew in Controller Area Networks. In *Proceedings of the 9th ACM/IEEE International Conference on Cyber-Physical Systems*, pages 32–42.

Van Herrewege, A., Singelee, D., and Verbauwhede, I. (2011). CANAuth: A Simple, Backward Compatible Broadcast Authentication Protocol for CAN Bus. In *ECRYPT Workshop on Lightweight Cryptography*.

A Time Shift Statistics

ID	# of Samples	Mean (ns)	Std. Dev. (ns)	Std. Dev (cm)
0x3ec	517	-62.9444	4.22815	12.6844
0x4d5	418	-62.9343	2.055	6.16499
0x778	4	-61.9638	1.18046	3.54139
0x352	510	2.049	1.69915	5.09745
0x288	10699	2.07594	2.4364	7.30919
0x4cb	510	2.08868	1.60234	4.80703
0x689	517	2.09483	0.915489	2.74647
0x102	16048	2.24681	3.74316	11.2295
0x106	16048	2.29587	4.15473	12.4642
0x4e2	486	2.3409	0.926301	2.7789
0x322	514	2.42082	3.01928	9.05785
0x29a	10025	2.55582	4.4946	13.4838
0x458	2563	41.6105	2.13171	6.39512
0x338	515	41.7426	1.85384	5.56153
0x4d4	473	41.7643	1.38032	4.14096
0x32c	516	41.7982	1.90502	5.71507
0x354	10630	68.0049	8.60718	25.8215
0x0c4	12685	68.6607	5.1656	15.4968
0x308	171	68.7487	4.02203	12.0661
0x623	2003	68.8762	1.30822	3.92467
0x420	510	68.8934	3.36012	10.0804
0x312	5957	68.9101	1.41566	4.24697
0x240	41765	68.9319	2.85064	8.55193
0x376	499	68.9321	1.44252	4.32757
0x0c0	31430	68.943	2.21871	6.65613
0x36e	1719	68.9499	2.13546	6.40639
0x08a	21659	68.9567	2.57982	7.73945
0x388	21789	68.9707	2.43622	7.30867
0x060	21255	68.9721	2.89066	8.67199
0x24e	31136	68.9772	2.40957	7.2287
0x154	42513	68.9832	1.95169	5.85508
0x168	21255	68.9871	2.42942	7.28826
0x378	499	68.9906	1.9579	5.8737
0x192	16069	68.9982	2.09111	6.27334
0x0a4	42528	69.0005	1.83936	5.51808
0x048	21255	69.0045	2.45669	7.37008
0x0a5	55028	69.0131	2.30028	6.90083
0x18c	16070	69.014	2.00657	6.0197
0x280	10600	69.0212	2.02714	6.08142
0x423	510	69.028	1.36729	4.10188
0x620	47568	69.029	1.14065	3.42196
0x360	513	69.0328	1.43671	4.31012
0x621	29903	69.0405	1.07903	3.23708
0x611	1923	69.0411	1.13658	3.40973
0x622	15774	69.0417	1.07541	3.22622
0x45c	146060	69.0443	1.11658	3.34975
0x610	40656	69.0465	1.1081	3.32431
0x624	6178	69.0514	1.06052	3.18156
0x3f2	2042	69.0523	1.38821	4.16462
0x328	1694	69.054	1.38745	4.16234
0x63b	28399	69.0576	1.06894	3.20683
0x627	514	69.0761	1.32297	3.96892
0x770	60	69.0913	1.40259	4.20778
0x678	1981	69.1175	1.147	3.441
0x30c	171	69.124	1.35414	4.06243
0x36c	511	69.1289	1.41421	4.24264
0x362	521	69.1365	1.44882	4.34647
0x7c6	28	69.1534	0.976756	2.93027
0x3cc	171	69.2481	1.38732	4.16197

Table A1: Statistics for Time Shift by ID